Int J Clin Exp Pathol 2017;10(10):10584-10592
www.ijcep.com /ISSN:1936-2625/IJCEP0040422

Original Article

Protective effect of TSG against oxygen-glucose deprivation in cardiomyoblast cell line H9c2: involvement of Bcl-2 family, Caspase 3/9, and Akt signaling pathway

Haiyang Xu, Jinghua Wang, Jingjing Zhang, Mingxian Li

The First Hospital of Jilin University, No. 71 Xinmin Street, Changchun 130021, Jilin, China

Received September 13, 2016; Accepted November 8, 2016; Epub October 1, 2017; Published October 15, 2017

Abstract: Objective: This study was designed to investigate the effect of TSG (2, 3, 5, 4'-tetrahydroxystibene-2-O-β-D-glucoside) on ischemic cardiomyopathy (ICM) related cell apoptosis and the mechanism related to it *in vitro*. Methods: Rat cardiomyoblast cell line H9c2 was cultured in oxygen-glucose withdrawal medium for 8 hours to establish an *in vitro* cell model of oxygen-glucose deprivation (OGD). Cells were pretreated with TSG to test the protective effect of it against OGD. Cell viability, apoptosis, mitochondrial transmembrane potential ($\Delta\Psi_m$), and apoptosis related proteins were detected using appropriated methods. Differences between treatments were analyzed. Results: OGD treatment inhibited cell viability, expression of Akt and Bax, induced loss of $\Delta\Psi_m$, cell apoptosis, and triggered expression of Bcl-2 and Caspase-3/9. TSG pretreatment, on the contrary, suppressed OGD-induced cell apoptosis, $\Delta\Psi_m$ loss, Bcl-2 and Caspase-3/9 expression, and promoted OGD-inhibited cell viability, Bax and Akt expression. Conclusion: We concluded that TSG's protective effect against OGD-induced *in vitro* ischemic cell model was associated to Akt/Caspase-3 pathway. TSG might be explored as a therapeutic target for ICM.

Keywords: TSG, oxygen-glucose deprivation, ischemic cardiomyopathy, cell apoptosis, Akt signaling

Introduction

Ischemic cardiomyopathy (ICM), a type of coronary heart disease (CHD), is a disturbance caused by multiple abnormal changes-induced cerebral vasculature occlusion [1, 2]. The occlusion of cerebral vasculature contributed to subsequently decreased delivery of glucose and oxygen to the brain that is oxygen-glucose deprivation (OGD), disruption of the ionic equilibrium (pH value) and calcium (Ca^{2+}) homeostasis, and eventual cell death [2, 3], thus ICM is an important cause of heart failure [4]. Duing to the complex causes and multiple disturbances, exploring of therapeutic treatment for ICM is a hard project.

During ICM progresses, or OGD, cerebral and heart cells are in oxygen-deficient environment, facilitating cell apoptosis or inhibiting cell viability, which is not conducive to patient survival and recovery [5]. Cell apoptosis is complex cellular function related to various factors, such as cell apoptosis related proteins Bcl-2 family, Akt and NF-κB signaling pathway, and mitochondrial transmembrane potential ($\Delta\Psi_m$) status [6-8]. For instance, Bcl-2 family, which consists of antiapoptotic proteins including Bcl-2, and proapoptotic proteins including Bax, promotes cell apoptosis via increase of Bcl-2 and decrease of Bax [6, 7]. Loss of $\Delta\Psi_m$ relates to cell apoptosis [9-11].

During the past decades, medicines and gene therapies applying to ICM treatment *in vivo*, *in vitro*, or in clinical practice, had been widespreadly reported, such as icariin, active flavonoid extracted from *Epimedium brevicornum* Maxim [12], resveratrol [13], tocilizumab [5], tetramethylpyrazine [14], and miR-210 inhibition [15]. All of these medicines had been proved to inhibiting OGD-induced cell apoptosis and increasing cell viability via regulating expression of Bcl-2 family proteins and related

signaling pathway [15], thus promoting recovery of ICM, *in vitro* by cell models or *in vivo* by animal models.

TSG (2, 3, 5, 4'-tetrahydroxystibene-2-O-β-D-glucoside), botanical extract ingredients extracted from traditional Chinese medicine Polygonum multiflorum [16], has protective effect on cell proliferation [17], and antioxidation [18]. However, few studies focusing on the TSG protective effect on OGD-induced cell apoptosis.

This study was designed to investigate the effect of TSG on OGD-induced cell apoptosis and the mechanism related to it, *in vitro*. H9c2 cells were treated with oxygen and glucose withdrawal medium to achieve *in vitro* OGD cell model. TSG pretreated to cells. Apoptotic related proteins and signaling pathways, cell viability, and apoptosis rates, and $\Delta\Psi_m$ were detected with appropriated methods. The effect of TSG on OGD-induced cell apoptosis was evaluated using statistical analysis. The potential of using TSG as the therapeutic treatment for ICM would be discussed.

Materials and methods

H9c2 cell culture and in vitro cell model establishment

A rat cardiomyoblast cell line H9c2 was purchased from ATCC (American Type Culture Collection, CRL-1446, Rattusnorvegicus, Rockville, MD, USA), cultured in DMEM (Dulbecco's modified Eagle's medium) supplementing with 10% FBS (Fetal bovine serum, Invitrogen, Carlsbad, CA, USA), 1% penicillin/streptomycin (Invitrogen).

OGD cell model was established to mimic ischemia by transferring cells to serum-glucose withdrawal DMEM in a InVivo 500 chamber (Ruskinn Life Science) supplemented anoxia air with 94% N_2/5% CO_2/1% O_2 at 37°C for 8 hours as described [19]. For TSG treatment, cells were pretreated with series TSG at 1, 2, 5, 10, 20, and 50 μM.

Model H9c2 cells pretreated with TSG or not and control cells were seeded in 24-well plates for series time points of 0, 6, 24 and 48 h. Subsequently, cells were additionally treated with solution of Cell Counting Kit 8 (CCK-8) assay (Sigma, St Louis, Mo, USA) for 2 h for absorbance at 450 nm (A450, Microplate spectrophotometer, Bio-Rad Labs, Hercules, CA, USA). For each experiment, three triplicates were performed and averaged value was calculated and reported as mean ± S.E (Standard Error) of three separate experiments.

Annexin V apoptosis assay

For cell apoptosis determination, cells were seeded in 6-well plates for 24 h and treated as experiments, and harvested by trypsin. Apoptotic cell and necrotic cell percentage determination was performed with Annexin V-FITC (Ann V) and propidium iodide (PI, Beckman Coulter, Fullerton CA, USA) staining assay. A total of 10,000 harvested cells were dark-labeled with AnnV and PI for 30 min followed by flow cytometry analysis (Becton Dickinson FACSCalibur™; FITC 530/30 and PI 585/42 nm).

Analysis of mitochondrial transmembrane potential ($\Delta\Psi_m$)

To analyse $\Delta\Psi_m$, a fluorescent dye of lipophilic cationic probe JC-1 (5, 5', 6, 6'-tetrachloro-1, 1', 3, 3'-tetraethylbenzimidazolcarbocyanine iodide, Molecular Probes, Eugene, OR, USA) was used and the JC-1 monomer/JC-1 dimer ratio was assessed as described [20]. In brief, 2×10^5 harvested H9c2 cells were adjusted to 1 mL volume with pre-warmed (37°C) culture medium, gently suspended with 2.5 μL of JC-1 dye (5 mg/ml in stock) and dark-incubated for 10 min at room temperature. After staining, cells were washed twice and resuspended with 1× PBS, and $\Delta\Psi_m$ collapse was examined and expressed as FL1-FITC fluorescence (JC-1 monomers, at 535 nm) versus FL2-PE fluorescence (JC-1 aggregates, at 590 nm).

Western blot analysis

Cellular proteins were extracted using RIPA lysis buffer (Solarbio, Beijing, China), measured using a micro BCA kit (Thermo Fisher Scientific Inc., MA, USA), separated by on 10% or 12% SDS-PAGE (Solarbio) and electro-transferred to polyvinylidene difluoride (PVDF) membranes (Invitrogen Corp., Carlsbad, CA, USA), blocked with 5% non-fat dry milk (BD Biosciences, Franklin Lakes, NJ, USA) for 1 h. Then, membranes were probed with the specific primary antibody overnight at 4°C (Caspases 9,

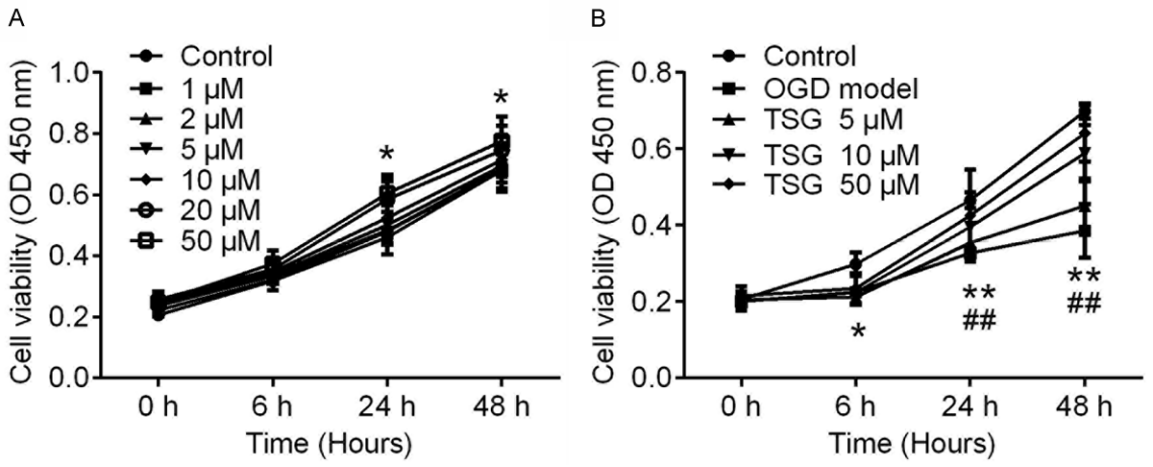

Figure 1. TSG attenuates oxygen-glucose deprivation-inhibited cell viability. CCK8 assay was used for cell viability determination. H9c2 cells were treated with TSG or OGD stimulus plus TSG pretreatment as described in experiments. All data were expressed as mean ± SE (Standard Error) of three separate experiments. * and **represents significant differences at $P < 0.05$ and $P < 0.01$, vs. control, respectively. # and ##represents significant differences at $P < 0.05$ and $P < 0.01$, vs. OGD, respectively.

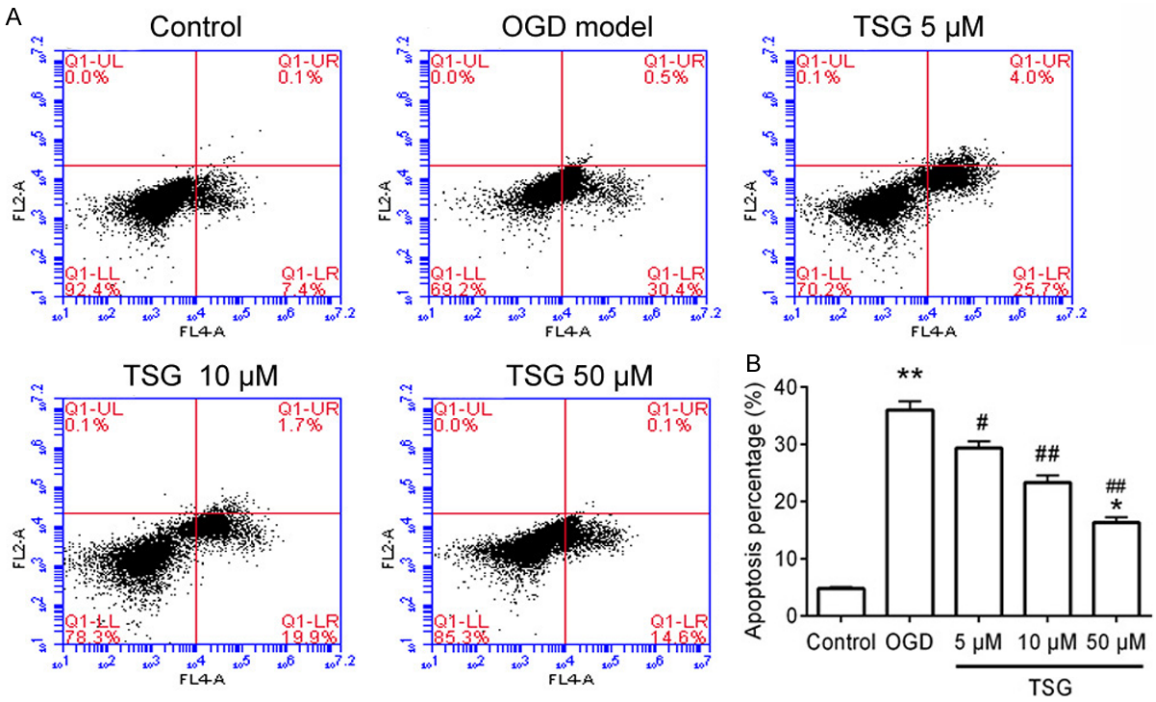

Figure 2. Detection of apoptosis cell was performed with Annexin V-FITC and PI staining assay. Cells were harvested by trypsin, labeled with Annexin V-FITC and PI and examined by flow cytometry. A total of 10,000 cells were analyzed from each sample. Percentages of early apoptosis cell (Annexin V+/PI-), late apoptosis cell (Annexin V+/PI+), necrosis cell (Annexin V-/PI+), and normal active cell (Annexin V-/PI-) were divided into four quadrants. A: Flow cytometry images; B: Statistical figure graphed using GraphPad Prism 6.0. Data were expressed as mean ± SE (Standard Error) of three separate experiments. * and **represents significant differences at $P < 0.05$ and $P < 0.01$, vs. control, respectively. # and ##represents significant differences at $P < 0.05$ and $P < 0.01$, vs. OGD, respectively.

Bcl-2, p-Akt, Akt, and GAPDH) or at room temperature for 120 min (activated Caspase 3, and Bax), followed by incubation with horseradish peroxidase-conjugated secondary antibody (1:1000) for 60 min at room temperature. Anti-activated Caspase 3 (1:500) and Caspase 9 (1:

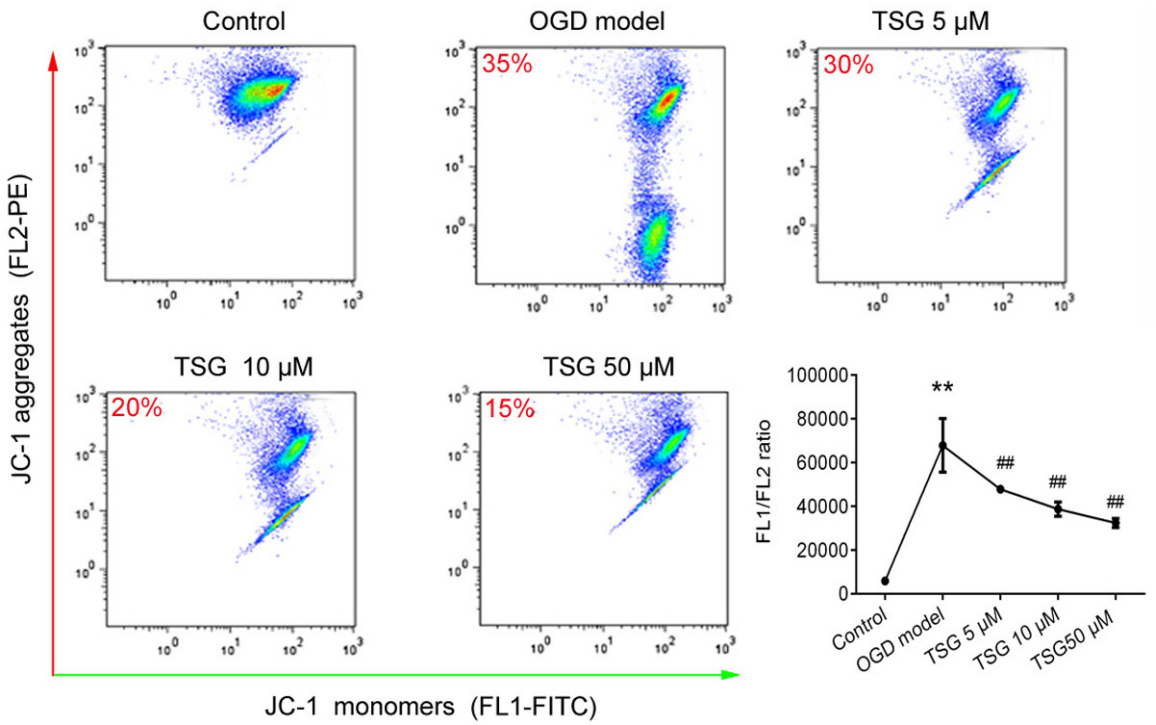

Figure 3. TSG blocks oxygen-glucose deprivation-induced loss of $\Delta\Psi_m$. Oxygen-glucose deprivation (OGD) induced apoptotic cells shows a loss of $\Delta\Psi_m$, showing a decrease in FL2 fluorescence (JC-1 aggregates) and a concomitant increase in FL1 fluorescence (JC-1 monomers). Statistical data were expressed as ratio of FL1/FL2 fluorescence (JC-1 monomer/aggregate ratio) from three separated experiments. Data were expressed as mean ± SE (Standard Error) of three separate experiments. * and **represents significant differences at $P < 0.05$ and $P < 0.01$, vs. control, respectively. # and ##represents significant differences at $P < 0.05$ and $P < 0.01$, vs. OGD, respectively.

1000) antibodies were purchased from Abcam Inc. (Cambridge, MA, USA). Anti-Bcl-2 (1:300) and Bax (1:300) antibodies were purchased from Santa Cruz Biotechnology (Santa Cruz, CA, USA). The other three antibodies anti-p-Akt (1:1000), Akt (1:1000) and GAPDH (1:2000) were obtained from Cell Signaling Technology (CST, Beverly, MA, USA). Blots were subjected to the enhanced chemiluminescence (ECL) detection system (Amersham Biosciences, Piscataway, NJ, USA), and quantitative analysis for band intensity was performed by adensitometry software QuantiScan (Biosoft Ferguson, MO, USA).

All statistical figures were analyzed and graphed using GraphPad Prism 6.0 (GraphPad Software Inc. La Jolla, CA) for windows, and all data were expressed as means ± SE of three separate experiments. The differences between two groups or more groups were analyzed using Student's unpaired t-test and one-way ANOVA, respectively. $P < 0.05$ was considered statistically significant.

Results

TSG attenuates OGD-inhibited cell viability

To study the effects of OGD stimulus or TSG therapy on cell viability, CCK8 assay was performed on cell line H9c2, exposed to culture conditions with oxygen-glucose withdrawal alone or together with TSG. **Figure 1A** shows that TSG administration alone markedly promoted cell viability with respect to the control cells ($P < 0.05$), in agreement with previous reports [21]. An opposite trend was found when cells were stimulated with OGD, showing a marker reduction in cell viability (**Figure 1B**). However, we could notice TSG triggered significant changes in cell viability of OGD cell model in a dose- and time-dependent manner ($P < 0.05$). These data suggested that OGD-simulated cell growth inhibition could be attenuated by TSG stimulation.

TSG inhibits OGD-triggered cell apoptosis

Since OGD inhibited cell viability as experiments showed, and some experimental mo-

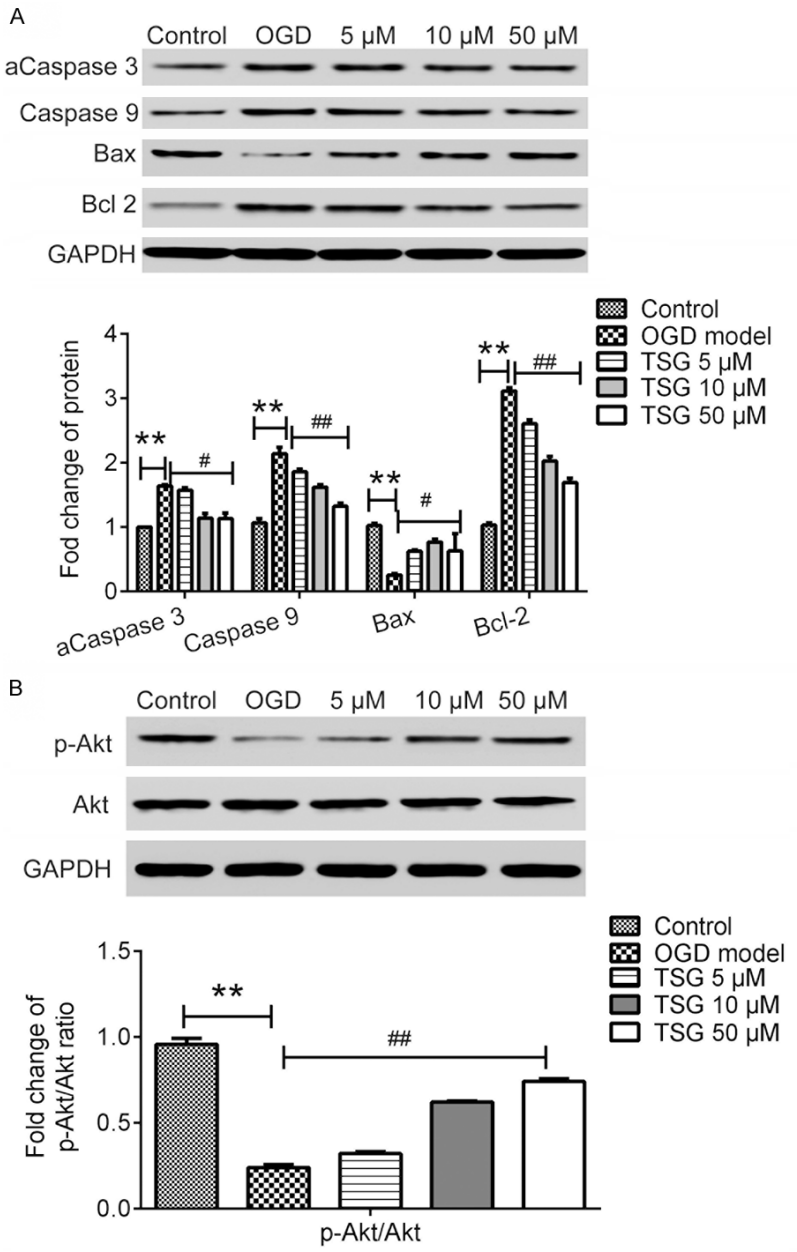

Figure 4. Expression of cell apoptosis related proteins and signaling pathway. A: Expression of Bcl-2 family proteins and Caspase-3/9 using Western blotting analysis. B: Akt signaling pathway. Cells were treated with OGD alone or plus TSG for 24 hours. * and **represents significant differences at $P < 0.05$ and $P < 0.01$, vs. control, respectively. # and ##represents significant differences at $P < 0.05$ and $P < 0.01$, vs. OGD, respectively.

dels revealed OGD activated cell death [13, 22], we tested the ability of OGD to induce apoptosis of H9c2 cells. We determined the maker increase in apoptotic cell percentage (Ann V+/PI-, early apoptosis and Ann V+/PI+, late apoptosis) of cells with oxygen-glucose withdrawal than controls ($P < 0.05$, **Figure 2**). Moreover, we observed decreases in apoptotic percentage of H9c2 cells with oxygen-glucose withdrawal together with TSG exposure, in TSG dose-dependent manner. These results revealed TSG protected cells against OGD activated cell death.

TSG blocks OGD stimulated changes on $\Delta\Psi_m$

As reported, loss or damage of $\Delta\Psi_m$ is a precipitating factor for cell apoptosis [23, 24], we speculated OGD damaged $\Delta\Psi_m$ and TSG's protective effect might benefit to blocking this damage. To address this speculation, we detected $\Delta\Psi_m$ using the fluorescent lipophilic cationic probe JC-1 and $\Delta\Psi_m$ collapse was expressed as FL1-FITC (JC-1 monomers)/FL2-PE (JC-1 aggregates) fluorescence. Results in **Figure 3** showed OGD markedly upregulated the JC-1 monomers/JC-1 aggregates fluorescence to over 11 times the control level ($P < 0.01$, **Figure 3**). OGD induced apoptotic cells showed a significant loss of $\Delta\Psi_m$, as a reduction in JC-1 aggregates accumulation (FL2 fluorescence) and a concomitant increase in JC-1 monomers accumulation (FL1 fluorescence). We next examined the effect of TSG protection on OGD-induced $\Delta\Psi_m$ damage. Results showed that TSG pretreatment of ischemic H9c2 cells blocked OGD-induced $\Delta\Psi_m$ damage, in a dose-dependent way, in an opposite trend to OGD stimulus showing an increase in JC-1 aggregates accumulation and a concomitant reduction in JC-1 monomers accumulation. These results sug-

gested TSG protected cells on OGD damaged $\Delta\Psi_m$, and this might benefit TSG's protective effect on cell apoptosis [24].

TSG suppresses OGD-simulated cell apoptosis via Bcl-2 family proteins and Akt signaling pathway

Bcl-2 family proteins, including Bcl-2 and Bax, play crucial roles in cell fate decision with active impact on caspases [3]. Akt takes vital part in cell survival and apoptosis via related signaling pathways such as P13K [25, 26]. Here we investigated the expression of Bcl-2 family proteins responded to ischemia *in vitro* in OGD cell model. We determined that H9c2 cells starved from oxygen and glucose increased the expression of activated Caspase 3, 9 and Bcl-2 to about 2~3 times the control level, and decreased the expression of Bax and p-Akt to one-third or one-fourth of the control (**Figure 4**). An opposite trend were observed in TSG pretreated cells, as TSG pretreatment inhibited OGD-triggered increase in Caspase 3, 9 and Bcl-2 expression and stimulated OGD-induced decrease in Bax and p-Akt expression, with dose-dependent way. These results determined that cell apoptosis in *in vitro* ischemia model associated with Bcl-2 family proteins expression and Akt signaling pathway inactivation.

Discussion

During cellular functions, various stimuli contribute to cellular death, among which including deprivation of serum, glucose, oxygen and cellular nutrients [3]. OGD is one stimulus make great influence on ICM. To illustrate the mechanism of OGD related cell apoptosis and involved signaling pathways, H9c2 cells were treated with medium lacked of oxygen and glucose to establish cell ischemic model *in vitro*. Cell apoptosis, $\Delta\Psi_m$ damage, expression of apoptosis related proteins and Akt signaling pathway activation were detected with appropriate methods. We concluded that OGD induced cell apoptosis related to dysregulation of Bcl-2 family proteins, and Caspase 3/9 elevation, agreed to previous reports [12, 15].

Apoptosis is the programmed cell death and its regulation involves in multiple factors including cell apoptosis related proteins such as Bcl-2 family proteins [12, 13], Caspase 3/9 [12, 27], and cellular signaling pathways such as Akt associated signaling pathway [28]. Bcl-2 family consists of antiapoptotic and proapoptotic proteins. Expression of antiapoptotic proteins, such as Bcl-2, inhibits cell apoptosis, and expression of proapoptotic proteins, such as Bax, promotes cell apoptosis [6, 7]. As reported, elevated Bax expression forms proapoptotic homodimers to activate Caspase-9 and subsequently apoptosis executor Caspase-3, while accumulated Bcl-2 proteins bands to Bax and forms heterodimers, therefore blocks Bax's proapoptotic effect [7, 12, 29]. In this present study, OGD treated H9c2 cells upregulated expression of a Caspase-3/9, proapoptotic protein Bcl-2, and cell apoptosis, inhibited antiapoptotic protein Bax and cell viability, suggesting the proapoptotic effect of OGD treatment. Moreover, TSG pretreatment annealed OGD-induced cell apoptotic related cellular dysregulation, revealing the antiapoptotic characteristics of TSG pretreatment and the therapeutic potential on ICM treatment. This was in accordance with results from other papers showing TSG's antiapoptotic activity [30].

Akt is a substrate of P13K/Akt antiapoptotic cascade. OGD decreased Akt phosphorylation [31]. Inhibitions of Akt signaling pathway and Caspase-3 cleavage are critical for cell apoptosis promotion [1]. In this study, we conformed that OGD induced inhibition of Akt and upregulation of Caspase-3 in H9c2 cells could be reversed by TSG pretreatment, revealing OGD promoted cell apoptosis via P13K/Akt/Caspase-3 signaling pathway and TSG's antiapoptotic activity was associated to P13K/Akt/Caspase-3 signaling pathway.

Cell apoptosis itself and OGD-induced cell apoptosis relates to damage of cell membranes and loss of $\Delta\Psi_m$ [9-11]. Loss or damage of $\Delta\Psi_m$ is a precipitating factor for cell apoptosis [23, 24]. $\Delta\Psi_m$ is widely recognized as a mitochondrial functional indicator [32]. OGD treatment triggered reactive oxygen species (ROS) production, early increase in intracellular Ca^{2+} uptake, which damage cellular membranes and related to cell apoptosis closely [33, 34]. Abnormal accumulation of ROS and intracellular Ca^{2+} challenged cellular ion structure balance, thus the intensity and permeability of cell cyto and plasma membranes, as well as mitochon-

drial permeability transition (MPT) and loss of $\Delta\Psi_m$ [35]. Moreover, opening of MPT pore (MPTP) is recognized critical determinant of ischemic-reperfusion injury, MPT and collapse of $\Delta\Psi_m$ by decreasing JC-1 aggregates and accumulating JC-1 monomers [36, 37]. The opening of MPTP and promotes its secondary effect on accelerating ROS production and ROS-induced damage on DNA fragmentation and cell necrosis [38]. OGD induce cell death and collapse of $\Delta\Psi_m$ were conformed by our research group and presented in this present study, this was in accordance with the reported results from other researches [10, 11]. Fatherly, we demonstrated TSG's protective ability against collapse of $\Delta\Psi_m$ by blocking OGD-induced decrease in JC-1 aggregates and increase o JC-1 monomers, suggesting TSG repaired OGD-destroyed intensity of cellular membranes.

Conclusion

In conclusion, our results clearly demonstrated that OGD-induced *in vitro* ischemic cell model apoptosis included decrease in cell viability, loss of $\Delta\Psi_m$, upregulation of Caspase-3, Caspase-9, and proapoptotic protein Bcl-2, and downregulation of antiapoptotic Bax and p-Akt. On the contrary, TSG's pretreated cells showed conversed results of these changes. TSG pretreatment increased cell viability, $\Delta\Psi_m$, downregulated Caspase-3, Caspase-9 and Bcl-2 expression, and upregulated Bax and p-Akt expression, in comparison to OGD treatment. This suggested that TSG's protective effect against OGD-induced *in vitro* ischemic cell model were associated to Akt/Caspase-3 pathway. In addition, these might shade light on TSG's potential therapeutic target for ICM.

Disclosure of conflict of interest

None.

Address correspondence to: Dr. Mingxian Li, The First Hospital of Jilin University, No. 71 Xinmin Street, Changchun 130021, Jilin, China. Tel: +86 0431 88782319. E-mail: mingxianli_1@126.com

References

[1] Xu YQ, Long L, Yan JQ, Wei L, Pan MQ, Gao HM, Zhou P, Liu M, Zhu CS, Tang BS, Wang Q. Simvastatin induces neuroprotection in 6-OHDA-lesioned PC12 via the PI3K/AKT/caspase 3 pathway and anti-inflammatory responses. Cns Neurosci Ther 2013; 19: 170-177.

[2] W L, FG S and O Y. Neuroprotective effect of apocynin nitrone in oxygen glucose deprivation-treated SH-SY5Y cells and rats with ischemic stroke. Tropical Journal of Pharmaceutical Research 2016; 15: 1681-1689.

[3] Bonavita F, Stefanelli C, Giordano E, Columbaro M, Facchini A, Bonafè F, Caldarera CM, Guarnieri C. H9c2 cardiac myoblasts undergo apoptosis in a model of ischemia consisting of serum deprivation and hypoxia: inhibition by PMA. Febs Lett 2003; 536: 85-91.

[4] Nagasaka T, Takama N and Kurabayashi M. Adaptive servo-ventilation therapy shows significant prevention of arrhythmias in patients with heart failure due to ischemic heart disease. Journal of the American College of Cardiology 2016; 67: 781-781.

[5] Wang S, Zhou J, Kang W, Dong Z, Wang H. Tocilizumab inhibits neuronal cell apoptosis and activates STAT3 in cerebral infarction rat model. Bosn J Basic Med Sci 2016; 16: 145-150.

[6] Ding J, Mooers BH, Zhang Z, Kale J, Falcone D, McNichol J, Huang B, Zhang XC, Xing C, Andrews DW, Lin J. After embedding in membranes antiapoptotic Bcl-XL protein binds both Bcl-2 homology region 3 and helix 1 of proapoptotic Bax protein to inhibit apoptotic mitochondrial permeabilization. J Biol Chem 2014; 289: 11873-96.

[7] Shamas-Din A, Kale J, Leber B, Andrews DW. Mechanisms of action of Bcl-2 family proteins. Cold Spring Harb Perspect Biol 2013; 5: a008714.

[8] Shukla V, et al. Phytoestrogen genistein inhibits EGFR/PI3K/NF-κB activation and induces apoptosis in human endometrial hyperplasial cells. Rsc Advances 2015; 5: 56075-56085.

[9] Circu ML, Aw TY. Glutathione and modulation of cell apoptosis. Biochim Biophys Acta 2012; 1823: 1767-77.

[10] Xu SY, Hu FY, Ren LJ, Chen L, Zhou ZQ, Zhang XJ, Li WP. Dantrolene enhances the protective effect of hypothermia on cerebral cortex neurons. Neural Regen Res 2015; 10: 1279-1285.

[11] Wang Y, Ma W, Jia A, Guo Q. Parecoxib protects mouse cortical neurons against OGD/R induced neurotoxicity by up-regulating Bcl-2. Neurochem Res 2015; 40: 1294-302.

[12] Mo ZT, Li WN, Zhai YR, Gong QH. Icariin Attenuates OGD/R-induced autophagy via Bcl-2-dependent cross talk between apoptosis and autophagy in PC12 cells. Evid Based

Complement Alternat Med 2016; 2016: 4343084.
[13] Huang T, Gao D, Jiang X, Hu S, Zhang L, Fei Z. Resveratrol inhibits oxygen-glucose deprivation-induced MMP-3 expression and cell apoptosis in primary cortical cells via the NF-κB pathway. Mol Med Rep 2014; 10: 1065-1071.
[14] Yang G, Qian C, Wang N, Lin C, Wang Y, Wang G, Piao X. Tetramethylpyrazine protects against oxygen-glucose deprivation-induced brain microvascular endothelial cells injury via Rho/Rho-kinase signaling pathway. Cell Mol Neurobiol 2016; [Epub ahead of print].
[15] Chio CC, Lin JW, Cheng HA, Chiu WT, Wang YH, Wang JJ, Hsing CH, Chen RM. MicroRNA-210 targets antiapoptotic Bcl-2 expression and mediates hypoxia-induced apoptosis of neuroblastoma cells. Arch Toxicol 2013; 87: 459-468.
[16] Deng T, et al. A dual-task method for the simultaneous detoxification and enrichment of stilbene glycoside from Polygonum multiflorum roots extract by macroporous resin. Chemical Engineering Journal 2014; 237: 138-145.
[17] Yi Z, et al. Effects and mechanisms of stilbene glucoside on the proliferation and collagen synthesis of cardiac fibroblasts stimulated by TGF-β1. Journal of China Pharmaceutical University 2014; 45: 362-367.
[18] Xiao-le X, et al. Effect of 2,3,4',5-tetrahydroxystilbene-2-O-β-D glucoside on proliferation and antioxidation of vascular smooth muscle cells. Chinese Pharmacological Bulletin 2010.
[19] Wang L, Pasha Z, Wang S, Li N, Feng Y, Lu G, Millard RW, Ashraf M. Protein kinase G1 α overexpression increases stem cell survival and cardiac function after myocardial infarction. PLoS One 2013; 8: e60087.
[20] Perelman A, Wachtel C, Cohen M, Haupt S, Shapiro H, Tzur A. JC-1: alternative excitation wavelengths facilitate mitochondrial membrane potential cytometry. Cell Death Dis 2012; 3: e430.
[21] Qin R, Li X, Li G, Tao L, Li Y, Sun J, Kang X, Chen J. Protection by tetrahydroxystilbene glucoside against neurotoxicity induced by MPP+: The involvement of PI3K/Akt pathway activation. Toxicol Lett 2011; 202: 1-7.
[22] Yan W, Chen Z, Chen J, Chen H. Isoflurane preconditioning protects rat brain from ischemia reperfusion injury via up-regulating the HIF-1α expression through Akt/mTOR/s6K activation. Cell Mol Biol (Noisy-le-Grand, France) 2016; 62: 38-44.
[23] Wani BA, Ramamoorthy D, Rather MA, Arumugam N, Qazi AK, Majeed R, Hamid A, Ganie SA, Ganai BA, Anand R, Gupta AP. Induction of apoptosis in human pancreatic MiaPaCa-2 cells through the loss of mitochondrial membrane potential (ΔΨm) by Gentiana kurroo root extract and LC-ESI-MS analysis of its principal constituents. Phytomedicine 2013; 20: 723-733.
[24] Selvaraj V, Armistead MY, Cohenford M, Murray E. Arsenic trioxide (As 2 O 3) induces apoptosis and necrosis mediated cell death through mitochondrial membrane potential damage and elevated production of reactive oxygen species in PLHC-1 fish cell line. Chemosphere 2013; 90: 1201-9.
[25] Shi J, Gu JH, Dai CL, Gu J, Jin X, Sun J, Iqbal K, Liu F, Gong CX. O-GlcNAcylation regulates ischemia-induced neuronal apoptosis through AKT signaling. Sci Rep 2014; 5: 14500.
[26] Fan QW and Weiss WA. Autophagy and Akt promote survival in glioma. Autophagy 2011; 7: 536-8.
[27] Jiang H, Zhang L, Liu J, Chen Z, Na R, Ding G, Zhang H, Ding Q. Knockdown of zinc finger protein X-linked inhibits prostate cancer cell proliferation and induces apoptosis by activating caspase-3 and caspase-9. Cancer Gene Ther 2012; 19: 684-9.
[28] Zhu Z, Sun H, Ma G, Wang Z, Li E, Liu Y, Liu Y. Bufalin induces lung cancer cell apoptosis via the inhibition of PI3K/Akt pathway. Int J Mol Sci 2012; 13: 2025-35.
[29] Sørensen BH, et al. Cell Signaling: Proteins, Pathways and Mechanisms: Downregulation of LRRC8A protects human ovarian and alveolar carcinoma cells against Cisplatin-induced expression of p53, MDM2, p21Waf1/Cip1, and Caspase-9/-3 activation. American Journal of Physiology Cell Physiology 2016; 310: C857-C873.
[30] Long SY, et al. Effect of TSG and PDTC on apoptosis of HUVECs induced by H_2O_2. Chinese Journal of Experimental Traditional Medical Formulae 2013.
[31] Ramírez-Sánchez J, Simões Pires EN, Nuñez-Figueredo Y, Pardo-Andreu GL, Fonseca-Fonseca LA, Ruiz-Reyes A, Ochoa-Rodríguez E, Verdecia-Reyes Y, Delgado-Hernández R, Souza DO, Salbego C. Neuroprotection by JM-20 against oxygen-glucose deprivation in rat hippocampal slices: involvement of the Akt/GSK-3β pathway. Neurochem Int 2015; 90: 215-223.
[32] Sha D, Wang Z, Qian L, Han Y, Zhang J, Gu S, Wang L, Li J, Chen C, Xu Y. A cocaine-regulated and amphetamine-regulated transcript inhibits oxidative stress in neurons deprived of oxygen and glucose. Neuroreport 2013; 24: 698-703.
[33] Cao ND and Kim JY. Exposure to electromagnetic field attenuates oxygen-glucose deprivation-induced microglial cell death by reduc-

ing intracellular Caand ROS. Int J Radiat Biol 2016; 92: 195-201.
[34] Pei Z, Zhu G, Huo X, Gao L, Liao S, He J, Long Y, Yi H, Xiao S, Yi W, Chen P, Li X, Li G, Zhou Y. CD24 promotes the proliferation and inhibits the apoptosis of cervical cancer cells in vitro. Oncol Rep 2016; 35: 1593-601.
[35] Kim JS, Wang JH, Lemasters JJ. Mitochondrial permeability transition in rat hepatocytes after anoxia/reoxygenation: role of Ca2+-dependent mitochondrial formation of reactive oxygen species. Am J Physiol Gastrointest Liver Physiol 2012; 302: G723-G731.
[36] Ong SB, Samangouei P, Kalkhoran SB, Hausenloy DJ. The mitochondrial permeability transition pore and its role in myocardial ischemia reperfusion injury. J Mol Cell Cardiol 2015; 78: 23-34.
[37] Lin HC, Lee TK, Tsai CC, Lai IR, Lu KS. Ischemic postconditioning protects liver from ischemia-reperfusion injury by modulating mitochondrial permeability transition. Transplantation 2012; 93: 265-71.
[38] Treulen F, Uribe P, Boguen R, Villegas JV. Mitochondrial permeability transition increases reactive oxygen species production and induces DNA fragmentation in human spermatozoa. Hum Reprod 2015; 30: 767-76.